JSLHR

Research Article

Anomalous White Matter Morphology in Adults Who Stutter

Matthew Cieslak,[a] Roger J. Ingham,[a] Janis C. Ingham,[a] and Scott T. Grafton[a]

Aims: Developmental stuttering is now generally considered to arise from genetic determinants interacting with neurologic function. Changes within speech-motor white matter (WM) connections may also be implicated. These connections can now be studied in great detail by high-angular-resolution diffusion magnetic resonance imaging. Therefore, diffusion spectrum imaging was used to reconstruct streamlines to examine white matter connections in people who stutter (PWS) and in people who do not stutter (PWNS).
Method: WM morphology of the entire brain was assayed in 8 right-handed male PWS and 8 similarly aged right-handed male PWNS. WM was exhaustively searched using a deterministic algorithm that identifies missing or largely misshapen tracts. To be abnormal, a *tract* (defined as all streamlines connecting a pair of gray matter regions) was required to be at least one 3rd missing, in 7 out of 8 subjects in one group and not in the other group.
Results: Large portions of bilateral arcuate fasciculi, a heavily researched speech pathway, were abnormal in PWS. Conversely, all PWS had a prominent connection in the left temporo-striatal tract connecting frontal and temporal cortex that was not observed in PWNS.
Conclusion: These previously unseen structural differences of WM morphology in classical speech-language circuits may underlie developmental stuttering.

The cause of developmental stuttering is still unknown, but it is generally considered to arise from a combination of genetic factors and subsequent alterations of neurologic function (Bloodstein & Ratner, 2008). It is also a disorder that varies across speaking situations and is often difficult to treat, especially after childhood (Bothe, Davidow, Bramlett, & Ingham, 2006). Brain imaging research initially highlighted abnormal neurophysiological activity in speech-motor and auditory-system brain regions among people who stutter (PWS; Alm, 2004; Brown, Ingham, Ingham, Laird, & Fox, 2005; De Nil, 2004).[1] But growing evidence of inconsistencies among the results of neurophysiological studies with PWS (see Ingham, Grafton, Bothe, & Ingham, 2012; Wymbs, Ingham, Ingham, Paolini, & Grafton, 2013)[2] and new capabilities in diffusion imaging have amplified interest in other pathophysiologic explanations. It has been hypothesized (see Wymbs et al., 2013) that there could be structural neuroanatomic differences in PWS based on generally more consistent brain imaging findings across studies (Chang, Erickson, Ambrose, Hasegawa-Johnson, & Ludlow, 2008; Cykowski et al., 2007; Foundas, Bollich, Corey, Hurley, & Heilman, 2001; Foundas et al., 2003; Jäncke, Hänggi, & Steinmetz, 2004; Mock et al., 2012). In particular, studies of white matter (WM) abnormalities have begun to emerge with magnetic resonance imaging (MRI) measures of diffusion, most commonly by diffusion tensor imaging (DTI) of PWS (Cai et al., 2014; Chang et al., 2008; Chang & Zhu, 2013; Connally, Ward, Howell, & Watkins, 2014; Cykowski, Fox, Ingham, Ingham, & Robin, 2010; Sommer, Koch,

[a]University of California, Santa Barbara
Correspondence to Roger J. Ingham: rjingham@speech.ucsb.edu
Editor: Jody Kreiman
Associate Editor: Hans-Georg Bosshardt
Received July 11, 2014
Revision received October 16, 2014
Accepted January 16, 2015
DOI: 10.1044/2015_JSLHR-S-14-0193

[1]Abbreviations: DSI, diffusion spectrum imaging; DTI, diffusion tensor imaging; FA, fractional anisotropy; LTPA, local termination pattern analysis; MRI, magnetic resonance imaging; PWS, person/people who stutter(s); PWNS, person/people who does/do not stutter; QSDR, *q*-space diffeomorphic reconstruction; SMS, Stuttering Measurement System; SPM, syllables per minute; WM, white matter; %SS, percentage of syllables stuttered.

[2]These inconsistencies have even occurred between findings from two recent meta-analyses of functional MRI and positron-emission tomography studies of stuttering (Belyk, Kraft, & Brown, 2015; Budde, Barron, & Fox, 2014). Both studies used an activation likelihood estimation (ALE) meta-analysis technique (Turkeltaub, Eden, Jones, & Zeffiro, 2002) with a sample-size correction (Eickhoff et al., 2009) on an overlapping (but not entirely identical) cluster of studies. There were some common findings, but Belyk et al. found abnormal activation of larynx and lip motor cortex to be a common occurrence, while Budde et al. found no such evidence. Conversely, Budde et al. reported the left red nucleus among the largest statistically converging areas, but red nucleus never emerged in the findings of Belyk et al.

Disclosure: *The authors have declared that no competing interests existed at the time of publication.*

Paulus, Weiller, & Büchel, 2002; Watkins, Smith, Davis, & Howell, 2008). Local changes of fractional anisotropy (FA) could reflect a loss of either structural integrity or organization in any WM connection passing through the suspect voxel. FA within each WM voxel has been compared between groups of PWS and people who do not stutter (PWNS). The most common observation is a reduction of FA in PWS, with large spatial variation across studies in the location of these differences (see Cai et al., 2014). Although not consistently, there have been some DTI studies among PWS, including children who stutter, demonstrating reduced FA or streamline counts in WM that probabilistically might include the left arcuate fasciculus (e.g., Chang & Zhu, 2013; Connally et al., 2014).

Differences in WM pathways such as the arcuate fasciculus suggest that, as with people experiencing many disease states and their clinicopathological sequelae, PWS may also be characterized by disconnections between important brain structures (Geschwind & Kaplan, 1962). However, the validity of WM findings based on DTI and derived FA values or streamline counts in PWS to date remains uncertain for a number of reasons. Most importantly, DTI is poorly suited for studying geometrically complex WM structures containing multiple crossing fiber bundles, as shown in Appendix A (Dick & Tremblay, 2012; Jones, Knösche, & Turner, 2013). The conventional level of inference for FA analysis treats each voxel independently. This creates a challenge in trying to conclude that a connection is abnormal when the FA results indicate small, isolated changes of diffusion. Because many intersecting WM bundles can pass through a given voxel, it is not always clear which might actually be involved. This is particularly important for mapping connectivity in speech-related pathways, such as the arcuate fasciculus, where there are extensive and complex crossing fibers (Verstynen, Badre, Jarbo, & Schneider, 2012). FA values are highly sensitive to the number of crossing fibers, and a reduction of FA does not necessarily assure that there is altered WM integrity. Furthermore, FA differences reported to date, while statistically significant, are based on very small effect sizes. Thus, DTI is insensitive for detecting definitive abnormalities in individual subjects. To overcome these limitations, we used a different MRI technique: diffusion spectrum imaging (DSI; Shin et al., 2012; Wedeen et al., 2008). DSI uses high angular resolution and multiple high *b* values to generate a dense, deterministic representation of diffusion in multiple orientations. From this, individual WM connections called streamlines are reconstructed. DSI is particularly valuable for minimizing error in fiber identification where there are crossing streamlines.

In addition to improving the underlying diffusion data, a map-reduce approach was employed that was similar to one that is popular in big-data analytics that circumvents the weaknesses of voxel-based comparisons of white matter (Figure 1; Cieslak & Grafton, 2014). In this framework, we define a WM tract as the set of all streamlines connecting a pair of predefined anatomical regions. The analysis allows for inference at the level of WM tracts by tabulating the spatial course of all streamlines in the brain that start and end in the same two gray matter regions. In this approach, the set of all streamlines connecting two regions forms a tract between the region pair. An exhaustive small-volume searchlight approach is applied over the WM. For each searchlight volume, the set of all gray matter pairs connected by any streamline is tabulated and the number of streamlines for each is recorded. Note that for any searchlight volume, it takes only one streamline to connect a pair of regions. Each searchlight was tested to see if there was any pair of connected regions largely present in one group but absent in the other group. If so, the center voxel of the sphere was labeled. This is an extremely conservative criterion, as the likelihood of this occurring by chance is .00076 (see Appendix B). In addition, it sets a very stringent criterion to label a connection as absent, as it requires only one connecting streamline to be present. The algorithm also tabulates the overall volume of each tract (the set of all streamlines connecting each pair of gray matter regions). In order to find only the most spatially robust differences between the groups, a difference was required to be present in at least one third of any tract's volume. The spatial extent of the presence or absence of these tracts was then plotted for each group.

Method

Participants

The participants for this study were volunteer male upper-division undergraduate and graduate students at the University of California, Santa Barbara. Each was paid for the time involved in this study. The study was approved by the university's Human Subjects Committee. The PWS were eight men (aged 20–29 years), and the PWNS were eight similarly aged men (20–31 years). Each PWS reported having a stuttering problem that began before the age of 6 years, and all had received some form of therapy during the last 10 years. All participants, both PWS and PWNS, had English as their first language, and all reported normal vision and hearing. PWS and PWNS were strongly right-handed as measured by the Edinburgh Handedness Inventory (score of more than +80; Oldfield, 1971).

Prior to the experiment, all participants' speech performance was assessed using three 3-min speaking tasks: oral reading, a self-selected monologue, and a telephone conversation. The assessments were made by two independent research assistants who had been trained on the Stuttering Measurement System (SMS; Ingham, Bakker, Ingham, Kilgo, & Moglia, 1999). Percentage of syllables stuttered (%SS) and syllables per minute (SPM) scores were obtained from audiovisual recordings for each participant during the three speaking tasks. The eight PWNS all produced zero stuttering on the speaking tasks and reported no history of a speech, language, or hearing problem. Other than stuttering, the eight PWS reported no history of a speech, language, or hearing problem, and none were observed by the clinician. The eight PWS (designated S1–S8),

whose stuttering ranged from mild to very severe, produced the following average scores across the three speaking tasks: S1, 5.5 %SS, 177 SPM; S2, 15.8 %SS, 102 SPM; S3, 8.1 %SS, 185 SPM; S4, 28.0 %SS, 88 SPM; S5, 4.8 %SS, 114 SPM; S6, 0.9 %SS, 169 SPM; S7, 0.8 %SS, 217 SPM; S8, 2.6 %SS, 161 SPM. The low-frequency stuttering by S6 and S7 was characterized by stuttering events of 4–6 s duration. Across the twenty-four 3-min speaking task recordings by the PWS and 24 by the PWNS, two research assistants, who scored all samples independently, did not differ by more than 7% in their total counts of stuttering events or syllables spoken per task. The average difference was 2.1% for counts of stuttering events and 1.4% for counts of syllables spoken.

Data Acquisition and Preprocessing

DSI and T1-weighted magnetization-prepared rapid gradient-echo scans were collected for each individual on a 3T Tim Trio scanner at the University of California, Santa Barbara Brain Imaging Center. The scans were acquired with the following parameters: TR = 2,300 ms, TE = 2.98 ms, flip angle = 9°, 3-D acquisition, field of view = (170, 240, 256 mm), matrix = 160 × 240 × 256. The DSI protocol sampled the entire brain, including cerebellum, along 257 directions using a Q5 half-sphere scheme, a maximum b value of 5,000 and a voxel size of 2.4 mm, axial acquisition, TR = 11.4 s, TE = 138 ms, 51 slices, field of view (231, 231, 123 mm), matrix = 96 × 96 × 51. The diffusion data were reconstructed using q-space diffeomorphic reconstruction (QSDR; Yeh & Tseng, 2011). QSDR is a two-step process whereby diffusion-weighted images are nonlinearly registered to the MNI152 FA volume using the Statistical Parametric Mapping package's nonlinear registration method, and spin density functions are then reconstructed in standard space. QSDR was performed using DSI Studio (http://www.dsi-studio.labsolver.org) with a mean diffusion distance of 1.25 mm. Fiber tracking was performed in DSI Studio using a cutoff angle of 55°, minimum length of 10 mm, and maximum length of 400 mm. Based on directional diffusion estimates from QSDR, fiber tracking was performed using a modified fiber-assignment-by-continuous-tracking algorithm until 100,000 streamlines had been reconstructed in each individual.

T1-weighted scans were segmented and parcellated into a set of anatomical regions using FreeSurfer's automated segmentation algorithm (version 5.0; Dale, Fischl, & Sereno, 1999). The Lausanne 2008 scale-60 atlas (generated by the connectomemapper v1.2; Gerhard et al., 2011; Hagmann et al., 2008) was used to parcellate cortex based on each individual's gyri and sulci, splitting them into equal-sized pieces along the primary axis of the gyrus. The scale-60 atlas produces 129 regions, including cortical and subcortical structures. This atlas was designed specifically for working with tractography data (Cammoun et al., 2012). Cortical and subcortical region labels were projected 4 mm into WM to account for streamlines that were not tracked through to gray matter. The same atlas dilation technique used by Cieslak and Grafton (2014) was employed.

WM Morphology Analysis

We compared the morphology of all WM tracts in the brain using the DSI2 package (https://github.com/mattcieslak/DSI2). We used the technique of local terminal pattern analysis (LTPA; Cieslak & Grafton, 2014) to perform these comparisons; the technique is graphically depicted in Figure 1. LTPA operates by exhaustively comparing spatially constrained subsets of streamlines between two groups. The subsets are generated by collecting from each individual all the streamlines that pass through a sphere in MNI space and grouping them by tract. Each tract is

Figure 1. Local termination pattern analysis (LTPA). Here we show an example connection in a 2-D brain (Panel a). The connection is defined by two terminal regions (Region A and Region B) and the streamlines connecting them from each individual (colored lines). Suppose there are three brains from the control group (PWNS) and three brains from the PWS group, and we want to test if there is a difference in this connection between the two groups. All three PWNS have streamlines connecting these regions, but only one of three PWS has a streamline connecting these regions. Five search spheres are constructed for illustrative purposes (colored squares). Panel b shows the result of searching in each sphere. Whether the individual has streamlines present or absent is designated by a check and an X, respectively. If the mXOR pattern is observed in that sphere, a large check is present in the bottom row. Panel c shows the result of searching over the entire connection for the mXOR pattern. All positive results are shaded in yellow.

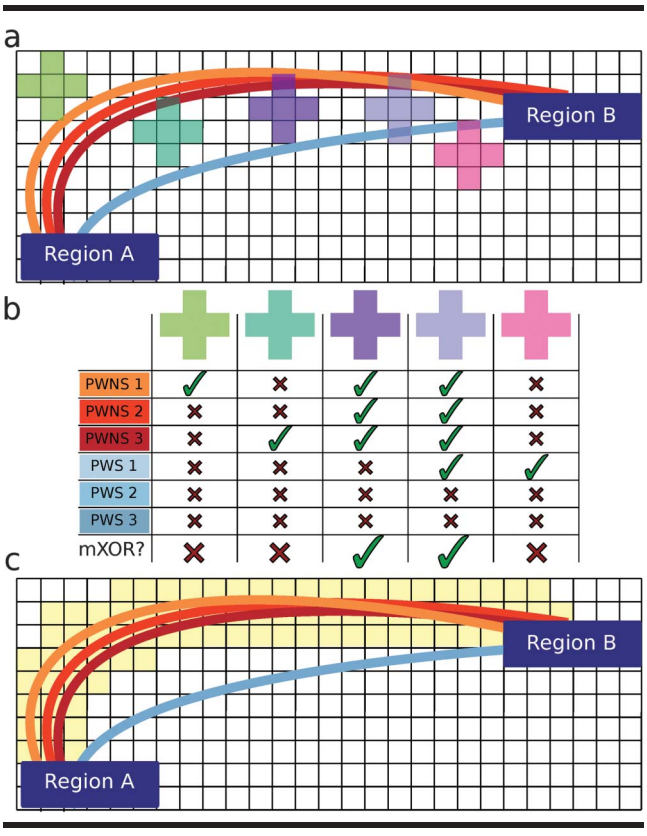

then compared to see if it is present in one population and absent in the other. The streamline comparison is performed with a stringent test, the modified exclusive "or" (mXOR), at every sphere in WM. The mXOR test allows one individual per group to deviate from the common pattern found in the group. For example, if seven or eight of eight PWS show a connection and seven or eight of eight PWNS do not show the connection, then the search yields a positive result for the connection at the search sphere's spatial location. Use of the mXOR test is ideally suited for this analysis. It is designed for two binary variables (PWS vs. PWNS, streamlines present vs. absent) and enables the derivation of expected false-positive and false-negative rates (see Appendix B). This is preferable to comparing stuttering behavior measures with a magnitude variable such as streamline count because (a) streamline count does not readily correspond to an interpretable physical quantity (Jones et al., 2013) and (b) the control group has no variance in the speech behavior measures.

Spheres are used instead of single voxels to prevent small anatomical differences from producing positive results. By using a 3-voxel search sphere, we allowed streamlines to differ by up to 6 mm without producing a positive result.

While the spatial and angular resolution are very high in these data, the number of individual observations is moderate. Due to this, an extraordinarily strict statistical test was used, which produces a false-positive result in 7.6 of every 10,000 spatial location comparisons and a false-negative rate of .89 (see Appendix B). To ensure a large effect size, we also required that at least one third of the tract's morphology differ between groups. Tract morphology difference was assessed by comparing each group's tract volume, which was calculated as the count of voxels intersected by the tract's streamlines. Any tract meeting these criteria was then subjected to a permutation test (10,000 permutations of group assignment) to assess significance post hoc.

Results

Three tracts passed our criteria for significance (see Figure 2). In PWS, the left arcuate fasciculus was missing a branch of streamlines that connect the left inferior temporal gyrus ($x = -47$, $y = -13$, $z = -29$; 1,302 ± 210 voxels) to the left insula ($x = -34$, $y = 11$, $z = 1$; 925 ± 76 voxels), with 39% of the tract volume missing compared to in PWNS, $p = .0015$. Also in PWS, the right arcuate fasciculus was missing a branch of streamlines that connect the inferior temporal gyrus ($x = 45$, $y = -11$, $z = -30$; 1,523 ± 218 voxels) to the supramarginal gyrus ($x = 49$, $y = -28$, $z = 30$; 1,704 ± 255 voxels), with 38% of the tract volume missing compared to in PWNS, $p = .0002$. In contrast, PWS showed a left temporo-striatal tract between the left inferior temporal gyrus ($x = -47$, $y = -14$, $z = -29$; 1,306 ± 2,264 voxels) and the left accumbens area ($x = -6$, $y = 6$, $z = -8$; 402 ± 75 voxels), with 46% greater tract volume than PWNS, $p < .00001$. Differences in tracts between the two groups cannot be attributed to differences in the morphology of the overlying cortical regions (see Figures 2A and 2B; see also the supplemental video for regions shown in 3-D).

Finally, the spatial coverage of region pairs with affected connectivity was statistically tested between groups to ensure that tract differences were not due to group differences in region labeling. Regional centers of mass were compared between groups using Hotelling's T^2 test (Winer, Brown, & Michels, 1991), and no significant differences were observed.

Discussion

The present DSI study provides strong evidence of differences between PWS and PWNS in morphology of WM connections known to be critical to speech production. Among the most important findings is the absence of streamlines in a large portion of the left arcuate tract connecting the insula and inferior temporal gyri in PWS, and also a part of the right arcuate tract connecting the inferior temporal and supramarginal gyrus in PWS. The findings also included the presence of a prominent connection in the left temporo-striatal tract connecting frontal and temporal cortex that was not observed in PWNS. These connections differentiated between PWS and PWNS who were matched for gender, age range, and handedness. Although this is a small study, it was conducted with eight PWS who displayed greatly different levels of severity of stuttering (see earlier),[3] and with a predefined large effect size within each individual. It is acknowledged that the present DSI study needs to be replicated across different populations of PWS, especially those who no longer stutter.

Previous DTI studies have found low FA values in regions approximating the arcuate fasciculus in the present study (Chang et al., 2008; Chang & Zhu, 2013; Connally et al., 2014; Cykowski et al., 2010; Sommer et al., 2002; Watkins et al., 2008). However, only Connally et al. (2014)

[3] In previous DTI studies, investigators have attempted to find correlations between WM abnormalities and stuttering severity. This introduces a number of problems that make such a correlation difficult to interpret. In the present study, the %SS data were derived from each participant's response to three different speaking tasks—oral reading, monologue, and telephone conversation. For most of the participants who stutter, scores across these tasks were very different. Some experienced more severe stuttering on the telephone task than on any other task, while some had more severe stuttering on the oral reading task than any other task. These data were also obtained on only one occasion and, quite predictably, were different on other occasions (e.g., during subsequent pretherapy sessions), thereby imperiling the validity of a correlation score derived from only one occasion. And of course, no speech performance data were obtained during the DSI scanning sessions. For these reasons, we believe it is hazardous to try to interpret a correlation between our %SS scores and WM. What the %SS data do show, however, is that each PWS did display stuttering across three widely used speaking tasks. It is worth noting that some previous attempts to find correlations between stuttering frequency or severity scores and WM have been generally unsuccessful (e.g., Cykowski et al., 2010; Chang et al., 2008)—probably for the aforementioned reasons.

Figure 2. (Panel a) Regions connected by tracts with a significant morphological difference between PWS and matched members of the control group. Common colors identify the terminating region locations. Voxels displayed here are a group result labeled as this region in at least one subject. Definitions of cortical regions in an individual were smaller than those shown here and never overlapped an individual segmentation. The region of the accumbens area was manually checked in each subject to make sure that the caudate had not been misidentified. (Panel b) Differences in tract morphology are highlighted by translucent spheres: Anatomy present in the control group and absent in the PWS group is highlighted by dark blue spheres, with maroon for the opposite. Multiple overlapping spheres appear opaque. Top: The left arcuate connection. Middle: The right arcuate connection. Bottom: The left temporo-striatal connection. All streamlines from all subjects are plotted in these images.

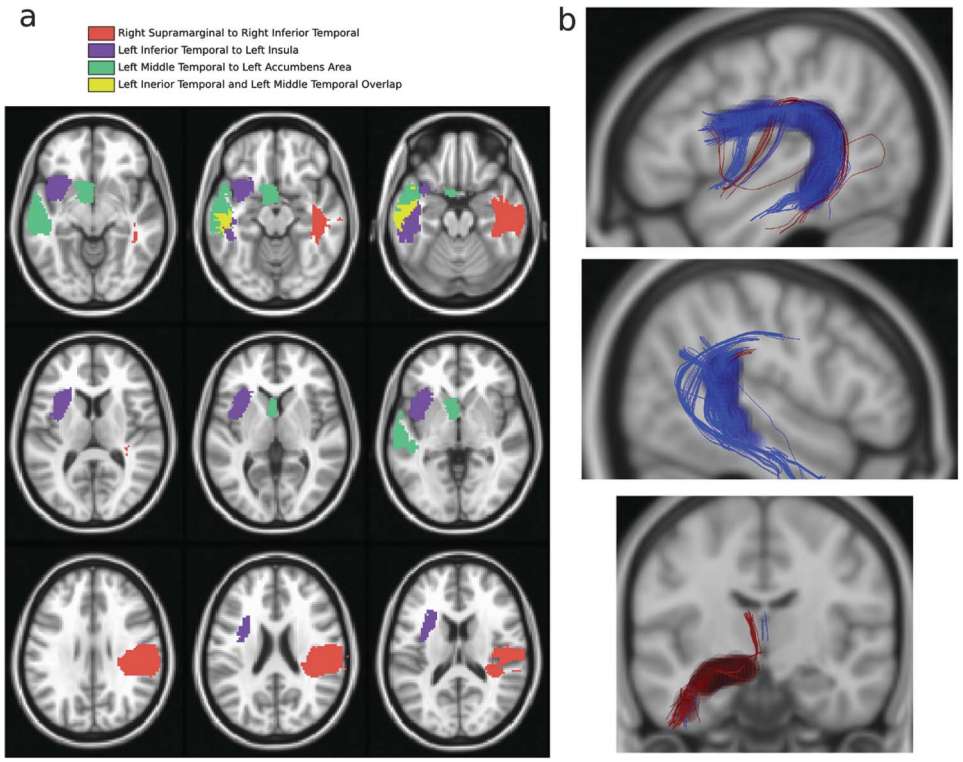

and Watkins et al. (2008) positioned low FA values over arcuate fasciculus bilaterally, as in the present study, and Cykowski et al. (2010) actually favored superior longitudinal fasciculus rather than arcuate fasciculus as the site of low FA values. Furthermore, no DTI study of PWS has reported evidence consistent with the presence of an excessive left temporo-striatal tract. However, it is difficult to draw direct comparisons between the findings of the present and previous diffusion studies on stuttering, because the differences between the DTI and DSI methodologies require comparisons between essentially incommensurate levels of measurement. As mentioned earlier, previous DTI studies have relied on very subtle FA differences to depict morphological differences; but FA values are difficult to interpret, particularly in areas where there are crossing fibers (e.g., arcuate fasciculus). Furthermore, an FA difference does not map to any specific change in morphology. Unlike the present study, none of these prior reports directly mapped the course of the arcuate fasciculus with a deterministic technique. In the present study, the DSI image acquisition method disambiguates crossing fibers, and the LTPA image analysis is able to assess the morphology of tracts by assessing the strength of connections between pairwise gray matter regions by using a systematic searchlight over the WM. Consequently, a strong inference can be made about the morphological differences between the PWS and control groups. It is certainly likely that some of the findings from DTI studies are partially reflected within the present DSI data.

Multiple studies have confirmed that the arcuate fasciculus has an essential role in normal speech production (Geschwind & Kaplan, 1962; but see Dick & Tremblay, 2012). There is also considerable evidence that damage or lesions in this pathway (Bernal & Ardila, 2009; Gillebert & Mantini, 2013) are associated with speech repetition aspects of conduction aphasia as well as related acquired speech disorders. Previous DTI studies of PWS (see earlier), based on average data, have also raised some doubts about the integrity of WM connections in PWS; however, this is the first study to document the complete absence of streamlines in most subjects within a significant part of a tract bilaterally. The relationship between clinical variability, stuttering severity, and this discovery needs to be elucidated with a larger sample, but this initial finding suggests that the absence of part of a tract corresponding to a well-known anatomical connection—the arcuate fasciculus—that is known to play

an integral role in normal speech production may have an important role in producing stuttered speech. Because these structures emerge during the second trimester of embryogenesis (Huang & Vasung, 2014; Kasprian et al., 2008), it seems reasonable to speculate that the unique changes in arcuate fasciculus in PWS might also arise during this period. The findings suggest a putative relationship between a structural connection that is formed in utero and a striking behavioral deficit that has a known genetic susceptibility (Kraft & Yairi, 2011). Furthermore, if it is agreed that the results of the previous DTI studies of stuttering have relevance to the present findings, then it is important to note that low probabilistic streamline counts have been reported in DTI studies on stuttering with children as young as 3 years (Chang & Zhu, 2013). They are unlikely to be by-products of years of stuttering. That would, in turn, add credence to the hypothesis that there is an embryogenic origin to these abnormal WM structures.

Using DTI-based probabilistic tractography in children who stutter, Chang and Zhu (2013) demonstrated reduced structural connectivity between the left pars opercularis and the middle temporal gyrus. In addition, they found reduced connectivity between the left superior temporal gyrus and middle frontal gyrus. While these reductions might be attributable to differences of the arcuate fasciculus, the primary connection between these lobes, the method used cannot distinguish the contribution of any particular WM tract. The present results help to reduce this uncertainty.

It is important to clarify that, based on our methodology, these results are not likely to be due to decreased WM integrity as estimated by DTI FA values. This is due to our use of quantitative anisotropy in fiber tracking (Yeh, Verstynen, Wang, Fernández-Miranda, & Tseng, 2013). If a fiber population shows any anisotropy above background noise, it will be available for use in tractography. Because no streamlines were produced, it indicates that no viable anisotropy exists along these tracts in the search spheres where we found group differences. If there are indeed fibers from these tracts present in these voxels, their microstructure is fundamentally different between groups. It is also important to consider the limitations that come with the strict test used in this study. In accepting a false-negative rate of .89, one cannot rule out the possibility that other WM connections form differences between these groups, in either integrity or morphology. However, this reduction in power provides strong assurance that the results reported here are not false positives.

Fiber tracking by any diffusion method is sensitive to the degree of myelination, the number of crossing fibers, and the presence and integrity of axons. With the DSI method and the use of orientation distribution functions to reconstruct streamlines, the ability to distinguish individual tracts, even in regions of significant fiber crossing, is greatly improved relative to conventional DTI scans (Wedeen et al., 2008). Our findings demonstrate a complete absence of streamlines in a major fraction of the arcuate fasciculus in seven of eight PWS. The extent, severity, and consistency of this absence of streamlines in a spatially compact section of WM are striking. Although it does not prove that there is an absence of axonal connections, it clearly points to a structural difference of some form between PWS and PWNS.

An equally important discovery was the consistent presence of a WM structure in the PWS group that occurred only inconsistently or not at all in the control group. This was a left temporo-striatal tract, which overlaps in part with the uncinate fasciculus. This suggests that this novel connection may contribute one or more potential functional roles. For example, Dick and Tremblay (2012, p. 3538) acknowledge the suggestive evidence of this WM tract's role in "auditory working memory/sound recognition," a fundamental requirement for speech production (see Guenther, 2006). Equally intriguing is the finding that the tract connects to left accumbens. The accumbens part of the striatum is particularly interesting because of recent evidence for its involvement in speech (Ackermann, Hage, & Ziegler, 2014). Excessive WM connections to ventral striatum (rather than the sensorimotor portion) may somehow emerge to compensate (or even overcompensate) for deficits in the arcuate fasciculus tract. Indeed, the fact that this excessive WM tract was not found in the homologous right area may also mean that that tract is functionally normal and potentially useful for certain therapy procedures. This additional WM structure in adult PWS could also be the result of inadequate pruning during the development of speech, along with possible excessive pruning or migration in the arcuate fasciculus (Chugani, 1998).

These patterns of WM projections might help to explain the difference between those who cease stuttering in childhood and those who develop persistent stuttering. The functional role of this abnormality needs to be considered in investigations of children who stutter and of PWS who show complete cessation of stuttering in adulthood.

Acknowledgments

The study was supported by National Institute on Deafness and Other Communication Disorders Grant DC007893 (awarded to R. J. Ingham), National Institute for Neurological Disease and Stroke Grant NS44393 (awarded to S. T. Grafton), and Institute for Collaborative Biotechnologies Contract W911NF-09-D-0001 from the U.S. Army Research Office (awarded to S. T. Grafton). We thank M. Ebrahimian, K. Paolini, K. Rein, and M. Mendoza for assistance with various parts of this study.

References

Ackermann, H., Hage, S. R., & Ziegler, W. (2014). Brain mechanisms of acoustic communication in humans and nonhuman primates: An evolutionary perspective. *Behavioral and Brain Sciences, 37,* 529–546.

Alm, P. A. (2004). Stuttering and the basal ganglia circuits: A critical review of possible relations. *Journal of Communication Disorders, 37,* 325–369.

Belyk, M., Kraft, S. J., & Brown, S. (2015). Stuttering as a trait or state—An ALE meta-analysis of neuroimaging studies. *European Journal of Neuroscience, 41,* 275–284. doi:10.1111/ejn.12765

Bernal, B., & Ardila, A. (2009). The role of the arcuate fasciculus in conduction aphasia. *Brain, 132,* 2309–2316.

Bloodstein, O., & Ratner, N. B (2008). *A handbook on stuttering* (6th ed.). Clifton Park, NY: Thomson Delmar.

Bothe, A. K., Davidow, J. H., Bramlett, R. E., & Ingham, R. J. (2006). Stuttering treatment research 1970–2005: I. Systematic review incorporating trial quality assessment of behavioral, cognitive, and related approaches. *American Journal of Speech-Language Pathology, 15,* 321–341.

Brown, S., Ingham, R. J., Ingham, J. C., Laird, A. R., & Fox, P. T. (2005). Stuttered and fluent speech production: An ALE meta-analysis of functional neuroimaging studies. *Human Brain Mapping, 25,* 105–117.

Budde, K. S., Barron, D. S., & Fox, P. T. (2014). Stuttering, induced fluency, and natural fluency: A hierarchical series of activation likelihood estimation meta-analyses. *Brain and Language, 139,* 99–107.

Cai, S., Tourville, J. A., Beal, D. S., Perkell, J. S., Guenther, F. H., & Ghosh, S. S. (2014). Diffusion imaging of cerebral white matter in persons who stutter: Evidence for network-level anomalies. *Frontiers in Human Neuroscience, 8,* 54. doi:10.3389/fnhum.2014.00054

Cammoun, L., Gigandet, X., Meskaldji, D., Thiran, J. P., Sporns, O., Do, K. Q., … Hagmann, P. (2012). Mapping the human connectome at multiple scales with diffusion spectrum MRI. *Journal of Neuroscience Methods, 203,* 386–397.

Chang, S.-E., Erickson, K. I., Ambrose, N. G., Hasegawa-Johnson, M. A., & Ludlow, C. L. (2008). Brain anatomy differences in childhood stuttering. *NeuroImage, 39,* 1333–1344.

Chang, S.-E., & Zhu, D. C. (2013). Neural network connectivity differences in children who stutter. *Brain, 136,* 3709–3726.

Chugani, H. T. (1998). A critical period of brain development: Studies of cerebral glucose utilization with PET. *Preventive Medicine, 27,* 184–188.

Cieslak, M., & Grafton, S. T. (2014). Local termination pattern analysis: A tool for comparing white matter morphology. *Brain Imaging and Behavior, 8,* 292–299.

Connally, E. L., Ward, D., Howell, P., & Watkins, K. E. (2014). Disrupted white matter in language and motor tracts in developmental stuttering. *Brain and Language, 131,* 25–35.

Cykowski, M. D., Fox, P. T., Ingham, R. J., Ingham, J. C., & Robin, D. A. (2010). A study of the reproducibility and etiology of diffusion anisotropy differences in developmental stuttering: A potential role for impaired myelination. *NeuroImage, 52,* 1495–1504.

Cykowski, M. D., Kochunov, P. V., Ingham, R. J., Ingham, J. C., Mangin, J.-F., Rivière, D., … Fox, P. T. (2007). Perisylvian sulcal morphology and cerebral asymmetry patterns in adults who stutter. *Cerebral Cortex, 18,* 571–583.

Dale, A. M., Fischl, B., & Sereno, M. I. (1999). Cortical surface-based analysis: I. Segmentation and surface reconstruction. *NeuroImage, 9,* 179–194.

De Nil, L. F. (2004). Recent developments in brain imaging research in stuttering. In B. Maassen, H. F. M. Peters, & R. Kent (Eds.), *Speech motor control in normal and disordered speech: Proceedings of the Fourth International Speech Motor Conference* (pp. 150–155). Oxford, England: Oxford University Press.

Dick, A. S., & Tremblay, P. (2012). Beyond the arcuate fasciculus: Consensus and controversy in the connectional anatomy of language. *Brain, 135,* 3529–3550.

Eickhoff, S. B., Laird, A. R., Grefkes, C., Wang, L. E., Zilles, K., & Fox, P. T. (2009). Coordinate-based activation likelihood estimation meta-analysis of neuroimaging data: A random-effects approach based on empirical estimates of spatial uncertainty. *Human Brain Mapping, 30,* 2907–2926. doi:10.1002/hbm.20718

Foundas, A. L., Bollich, A. M., Corey, D. M., Hurley, M., & Heilman, K. M. (2001). Anomalous anatomy of speech-language areas in adults with persistent developmental stuttering. *Neurology, 57,* 207–215.

Foundas, A. L., Corey, D. M., Angeles, V., Bollich, A. M., Crabtree-Hartman, E., & Heilman, K. M. (2003). Atypical cerebral laterality in adults with persistent developmental stuttering. *Neurology, 61,* 1378–1385.

Gerhard, S., Daducci, A., Lemkaddem, A., Meuli, R., Thiran, J.-P., & Hagmann, P. (2011). The Connectome Viewer Toolkit: An open source framework to manage, analyze, and visualize connectomes. *Frontiers in Neuroinformatics, 5,* 3.

Geschwind, N., & Kaplan, E. (1962). A human cerebral deconnection syndrome. *Neurology, 12,* 675–685.

Gillebert, C. R., & Mantini, D. (2013). Functional connectivity in the normal and injured brain. *The Neuroscientist, 19,* 509–522.

Guenther, F. H. (2006). Cortical interactions underlying the production of speech sounds. *Journal of Communication Disorders, 39,* 350–365.

Hagmann, P., Cammoun, L., Gigandet, X., Meuli, R., Honey, C. J., Wedeen, V. J., & Sporns, O. (2008). Mapping the structural core of human cerebral cortex. *PLOS Biology, 6,* e159. doi:10.1371/journal.pbio.0060159

Huang, H., & Vasung, L. (2014). Gaining insight of fetal brain development with diffusion MRI and histology. *International Journal of Developmental Neuroscience, 32,* 11–22.

Ingham, R. J., Bakker, K., Ingham, J. C., Kilgo, M., & Moglia, R. (1999). Stuttering Measurement System [Computer software]. Santa Barbara: Department of Speech and Hearing Sciences, University of California, Santa Barbara. Retrieved from http://www.speech.ucsb.edu/

Ingham, R. J., Grafton, S. T., Bothe, A. K., & Ingham, J. C. (2012). Brain activity in adults who stutter: Similarities across speaking tasks and correlations with stuttering frequency and speaking rate. *Brain and Language, 122,* 11–24.

Jäncke, L., Hänggi, J., & Steinmetz, H. (2004). Morphological brain differences between adult stutterers and non-stutterers. *BMC Neurology, 4,* 23–30.

Jones, D. K., Knösche, T. R., & Turner, R. (2013). White matter integrity, fiber count, and other fallacies: The do's and don'ts of diffusion MRI. *NeuroImage, 73,* 239–254.

Kasprian, G., Brugger, P. C., Weber, M., Krssák, M., Krampl, E., Herold, C., & Prayer, D. (2008). In utero tractography of fetal white matter development. *NeuroImage, 43,* 213–224.

Kraft, S. J., & Yairi, E. (2011). Genetic bases of stuttering: The state of the art, 2011. *Folia Phoniatrica et Logopaedica, 64,* 34–47.

Mock, J. R., Zadina, J. N., Corey, D. M., Cohen, J. D., Lemen, L. C., & Foundas, A. L. (2012). Atypical brain torque in boys with developmental stuttering. *Developmental Neuropsychology, 37,* 434–452.

Oldfield, R. C. (1971). The assessment and analysis of handedness: The Edinburgh Inventory. *Neuropsychologia, 9,* 97–113.

Shin, S. S., Verstynen, T., Pathak, S., Jarbo, K., Hricik, A. J., Maserati, M., … Schneider, W. (2012). High-definition fiber tracking for assessment of neurological deficit in a case of traumatic brain injury: Finding, visualizing, and interpreting small sites of damage [Case report]. *Journal of Neurosurgery, 116,* 1062–1069.

Sommer, M., Koch, M. A., Paulus, W., Weiller, C., & Büchel, C. (2002). Disconnection of speech-relevant brain areas in persistent developmental stuttering. *The Lancet, 360,* 380–383.

Turkeltaub, P. E., Eden, G. F., Jones, K. M., & Zeffiro, T. A. (2002). Meta-analysis of the functional neuroanatomy of single-word reading: Method and validation. *NeuroImage, 16,* 765–780. doi:10.1006/nimg.2002.1131

Verstynen, T. D., Badre, D., Jarbo, K., & Schneider, W. (2012). Microstructural organizational patterns in the human corticostriatal system. *Journal of Neurophysiology, 107,* 2984–2995.

Watkins, K. E., Smith, S. M., Davis, S., & Howell, P. (2008). Structural and functional abnormalities of the motor system in developmental stuttering. *Brain, 131,* 50–59.

Wedeen, V. J., Wang, R. P., Schmahmann, J. D., Benner, T., Tseng, W. Y. I., Dai, G., … de Crespigny, A. J. (2008). Diffusion spectrum magnetic resonance imaging (DSI) tractography of crossing fibers. *NeuroImage, 41,* 1267–1277.

Winer, B. J., Brown, D. R., & Michels, K. M. (1991). *Statistical principles in experimental design* (3rd ed.). New York, NY: McGraw-Hill.

Wymbs, N. F., Ingham, R. J., Ingham, J. C., Paolini, K. E., & Grafton, S. T. (2013). Individual differences in neural regions functionally related to real and imagined stuttering. *Brain and Language, 124,* 153–164.

Yeh, F.-C., & Tseng, W.-Y. I. (2011). NTU-90: A high angular resolution brain atlas constructed by q-space diffeomorphic reconstruction. *NeuroImage, 58,* 91–99.

Yeh, F.-C., Verstynen, T. D., Wang, Y., Fernández-Miranda, J. C., & Tseng, W.-Y. I. (2013). Deterministic diffusion fiber tracking improved by quantitative anisotropy. *PLOS ONE, 8,* e80713. doi:10.1371/journal.pone.0080713

Appendix A

Supplemental Figures

Figure A1. Diffusion imaging works by estimating the diffusivity of water along a set of directions (represented as arrows in the left column of images), sometimes at a number of magnetic gradient strengths (represented by colors on the left columns images). **Upper Left**: The directions are typical for a diffusion tensor imaging (DTI) scan where diffusion is all sampled at one gradient strength. **Lower Left:** The sampling scheme from diffusion spectrum imaging (DSI). This DSI scan samples 257 directions over a range of different gradient strengths. The effects of increased angular sampling resolution can be seen by comparing the resulting tractography based on the two diffusion sampling techniques (right column). In this example, we show tractography at a triple-crossing within the white matter of the parietal lobe. **Upper Right:** DTI-based tractography produces multiple spurious streamline bundles that do not cross. **Lower Right**: DSI-based resolves the triple crossing.

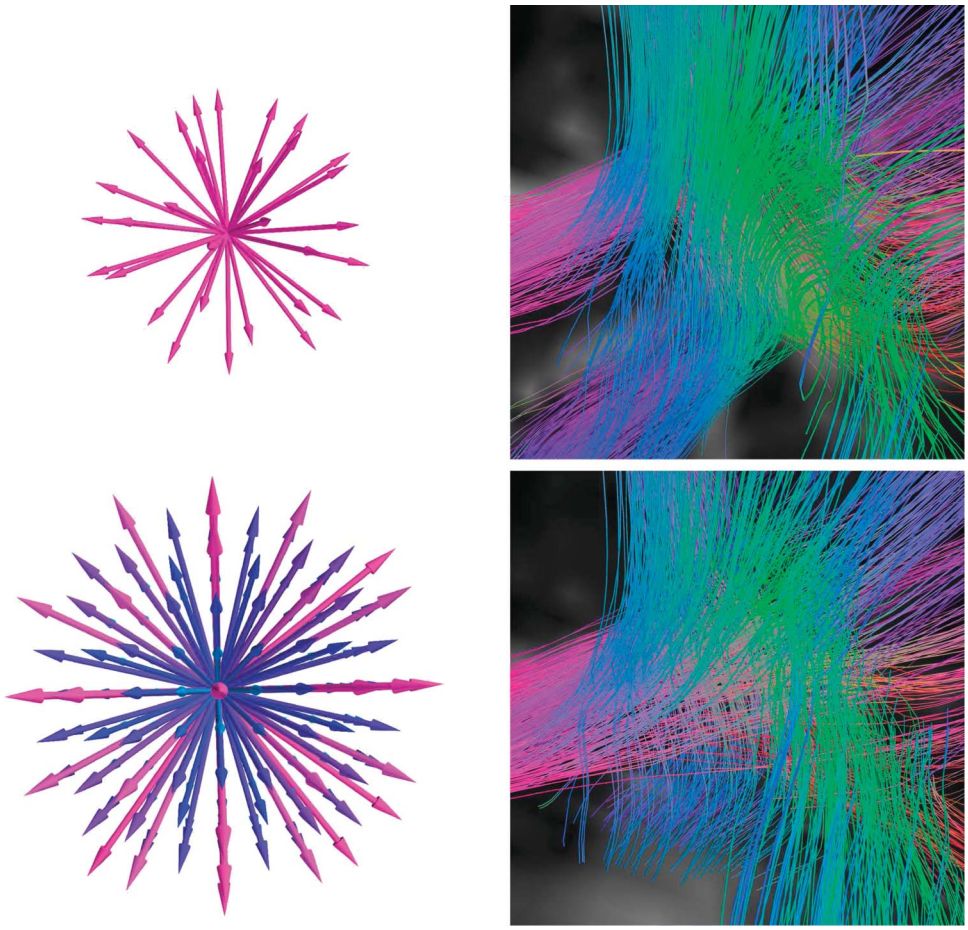

Appendix B

Statistical Null Model

Let the frequency of a tract existing in a population in a search sphere be θ. In the control group it is θ_c, and in PWS, θ_s. We want to convincingly show that $\theta_c \neq \theta_s$. However, all we are able to observe is our data set of eight PWS and eight PWNS. Let the condition where seven or eight PWS have the connection present be denoted as s_+, and the condition where it is absent in seven or eight PWS be s_-. When seven or eight men in the control group have the connection present, it is denoted as c_+; when it is absent, c_-.

$$p(c_+) = \theta_c^8 + \binom{8}{7}\theta_c^7(1-\theta_c)p(c_-) = (1-\theta_c)^8 + \binom{8}{7}\theta_c(1-\theta_c)^7 p(s_+) = \theta_s^8 + \binom{8}{7}\theta_s^7(1-\theta_s)$$

$$p(s_-) = (1-\theta_s)^8 + \binom{8}{7}\theta_s(1-\theta_s)^7$$

For a Type I error to occur, it is the case that an mXOR test is passed even though $\theta_c = \theta_s$. There are two ways this could occur: if all the PWS have the connection in the search sphere and no members of the control group do (c_-, s_+), or if all the members of the control group have the connection in the search sphere and none of the PWS do (c_+, s_-). We can determine the probability of a false positive α as a function of θ:

$$\alpha(\theta_c, \theta_s) = p(c_+)p(s_-) + p(c_-)p(s_+).$$

By solving $\int_{\theta=0}^{\theta=1} \alpha(\theta,\theta)$, we can calculate the false-positive rate to be .00076. We can also solve for the false-negative rate by evaluating

$$\beta = \int_{\theta_s=0}^{\theta_s=1}\int_{\theta_c=0}^{\theta_c=1} 1 - \alpha(\theta_c, \theta_s),$$

which we solved numerically, yielding β = .89. In other words, we are unable to detect all but the strongest 11% of real differences.

Permutation Testing

To test the validity of the null model, we performed permutation tests. We generated 10,000 unique permutations of the labels assigned to subjects ("PWS" or "control group") and applied them to the data such that any mXOR observed is a false positive as far as the analysis of PWS versus control group is concerned. We ran the same LTPA test using these permuted labels to calculate an empirical false-positive rate. The rate observed was .00071, very close to what we derived in the foregoing. In this article, *p* values reported are exact *p* values from the permutation test.